

Earthquakes in Switzerland and surrounding regions during 2013

Tobias Diehl · John Clinton · Toni Kraft · Stephan Husen · Katrin Plenkers ·
Aurélié Guilhem · Yannik Behr · Carlo Cauzzi · Philipp Kästli ·
Florian Haslinger · Donat Fäh · Clotaire Michel · Stefan Wiemer

Received: 6 September 2014 / Accepted: 30 September 2014 / Published online: 21 October 2014
© Swiss Geological Society 2014

Abstract This report of the Swiss Seismological Service summarizes the seismic activity in Switzerland and surrounding regions during 2013. During this period, 699 earthquakes and 208 quarry blasts were detected and located in the region under consideration. With a total of 18 events with local magnitudes $M_L \geq 2.5$, the seismic activity in the year 2013 was slightly below the average over the previous 38 years. Most noteworthy were the two earthquake sequences of St. Gallen (SG) in July and Balzers (FL) in December. The former was induced by reservoir stimulation operations at the St. Gallen geothermal project. The maximum local magnitude in the sequence was 3.5, comparable in size with the M_L 3.4 event induced by stimulation operations below Basel in 2006. The sequence of Balzers was associated with an M_L 4.1 earthquake in the border region to Liechtenstein. More than 30 aftershocks with magnitudes ranging between $M_L -0.2$ and M_L 3.7 were detected in the month following the mainshock. The M_L 3.5 St. Gallen and the M_L 4.1 Balzers earthquakes were widely felt by the public but no reports on damages are known. The maximum intensity for both events was IV.

Keywords Seismicity · Induced seismicity · Focal mechanisms · Seismotectonics · St. Gallen · Balzers

Editorial handling: A. G. Milnes.

T. Diehl (✉) · J. Clinton · T. Kraft · S. Husen · K. Plenkers ·
A. Guilhem · Y. Behr · C. Cauzzi · P. Kästli · F. Haslinger ·
D. Fäh · C. Michel · S. Wiemer
Swiss Seismological Service, ETH Zürich, Sonneggstrasse 5,
8092 Zurich, Switzerland
e-mail: tobias.diehl@sed.ethz.ch
URL: <http://www.seismo.ethz.ch>

Zusammenfassung Dieser Bericht des Schweizerischen Erdbebendienstes stellt eine Zusammenfassung der im Vorjahr in der Schweiz und Umgebung aufgetretenen Erdbeben dar. Im Jahr 2013 wurden im erwähnten Gebiet 699 Erdbeben sowie 208 Sprengungen erfasst und lokalisiert. Mit 18 Beben der Magnitude $M_L \geq 2.5$, lag die seismische Aktivität im Jahr 2013 leicht unter dem Durchschnitt der vorhergehenden 38 Jahre. Die bedeutendsten Ereignisse waren die zwei Erdbebensequenzen von St. Gallen (SG) im Juli und Balzers (FL) im Dezember. Die Sequenz von St. Gallen wurde durch Stimulationsmassnahmen in Reservoiregesteinen im Rahmen des Geothermieprojekts der Stadt St. Gallen induziert. Die maximale Magnitude innerhalb der Sequenz war M_L 3.5, welche vergleichbar ist mit der des induzierten M_L 3.4 Bebens von Basel im Jahr 2006. Die Erdbebensequenz von Balzers steht im Zusammenhang mit einem M_L 4.1 Beben in der Grenzregion zu Liechtenstein. Mehr als 30 Nachbeben mit Magnituden zwischen $M_L -0.2$ und M_L 3.7 wurden im ersten Monat nach dem Hauptbeben registriert. Das M_L 3.5 Beben von St. Gallen und das M_L 4.1 Beben von Balzers wurden von der Bevölkerung weiträumig verspürt, Schäden wurden aber nicht berichtet. Die maximale Erschütterung bei beiden Beben lag im Bereich der Intensität IV.

Resumé Ce rapport du Service Sismologique Suisse résume l'activité sismique en Suisse et dans ses régions environnantes au cours de l'année 2013. Pendant cette période, 699 tremblements de terre et 208 tirs de carrière ont été détectés et localisés dans la région étudiée. Avec un total de 18 évènements de magnitude $M_L \geq 2.5$, l'activité sismique de l'année 2013 est légèrement

inférieure à la moyenne enregistrée au cours des 38 dernières années. Les deux séquences sismiques les plus remarquables sont celles de Saint Gall (SG) en juillet et de Balzers (FL) en décembre 2013. La première a été induite par les opérations associées à la stimulation du réservoir dans le cadre du projet d'activité géothermique de St Gall. La plus forte magnitude locale de la séquence était 3.5, ce qui est comparable en taille avec le séisme de M_L 3.4 induit par les activités de stimulation sous la ville de Bâle en 2006. La séquence de Balzers était, elle, associée à un séisme de magnitude locale 4.1 à la frontière avec le Liechtenstein. Plus de 30 répliques sismiques avec des magnitudes comprises entre -0.2 et 3.7 ont été détectées dans le mois qui a suivi le choc principal. Les tremblements de terre de St Gall (M_L 3.5) et Balzers (M_L 4.1) ont été largement ressentis par la population. Néanmoins aucun dommage n'a été rapporté. L'intensité maximale enregistrée pour chacun des deux séismes était de IV.

1 Introduction

Past earthquake activity in and around Switzerland has been documented in an uninterrupted series of annual reports from 1879 until 1963 (*Jahresberichte des Schweizerischen Erdbebendienstes*). Three additional annual reports have been published for the years 1972–1974. These reports together with historical records of earthquakes dating back to the thirteenth century were summarized by Pavoni (1977) and provided the basis for the first seismic hazard map of Switzerland (Sägesser and Mayer-Rosa 1978). With the advent of routine data processing by computer, the wealth of data acquired by the nationwide seismograph network has been regularly documented in bulletins with detailed lists of all recorded events (*Monthly Bulletin of the Swiss Seismological Service*). Since 1996, annual reports summarizing the seismic activity in Switzerland and surrounding regions have been published in the present form (Baer et al. 1997, 1999, 2001,

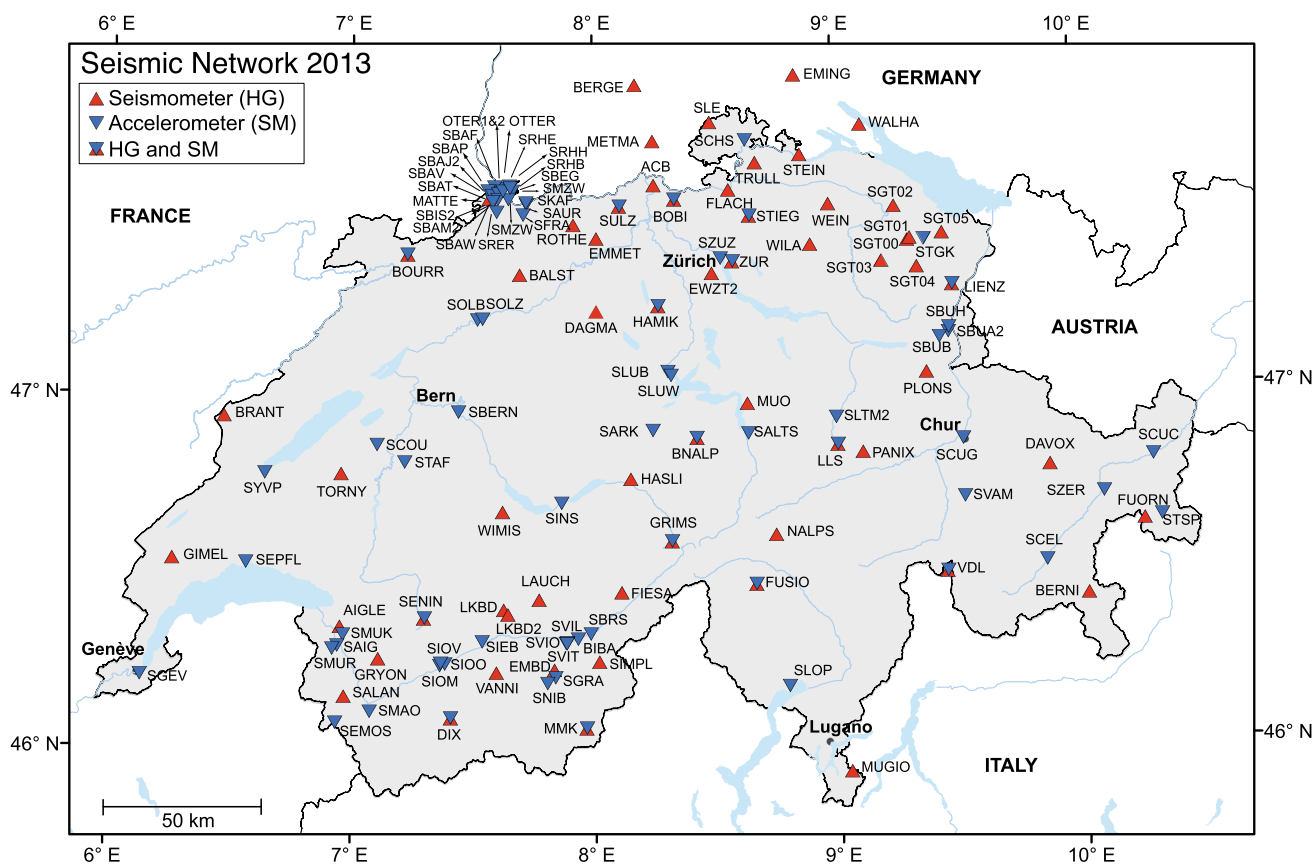


Fig. 1 Seismograph stations in Switzerland with on-line data acquisition operational at the end of 2013. The stations defined as high-gain (HG) are mostly equipped with broad-band or 5-s sensors, whereas

the strong-motion stations (SM) are accelerometers (see also Table 4, 5, 6 in “Appendix”)

2003, 2005, 2007; Deichmann et al. 1998, 2000a, 2002, 2004, 2006, 2008, 2009, 2010, 2011, 2012; Diehl et al. 2013). In the course of reassessing the seismic hazard in Switzerland, a uniform earthquake catalogue covering both the historical and instrumental periods was compiled in 2002 (Fäh et al. 2003). The official seismic hazard map of Switzerland based on this catalogue was released in 2004 (Giardini et al. 2004; Wiemer et al. 2009). In 2009, the Earthquake Catalogue of Switzerland was revised (ECOS-09) and is now available on-line (<http://www.seismo.ethz.ch/prod/catalog/index>). In addition, numerous studies covering different aspects of the recent seismicity of Switzerland have been published in the scientific literature

(for overviews and additional references see, e.g. Deichmann 1990; Pavoni and Roth 1990; Rüttener 1995; Rüttener et al. 1996; Pavoni et al. 1997; Deichmann et al. 2000b; Kastrop et al. 2004; 2007; Husen et al. 2007; Marschall et al. 2013, Singer et al. 2014).

2 Data acquisition and analysis

2.1 Seismic stations in operation during 2013

The Swiss Seismological Service (*Schweizerischer Erdbebendienst*, SED) operates two separate nationwide

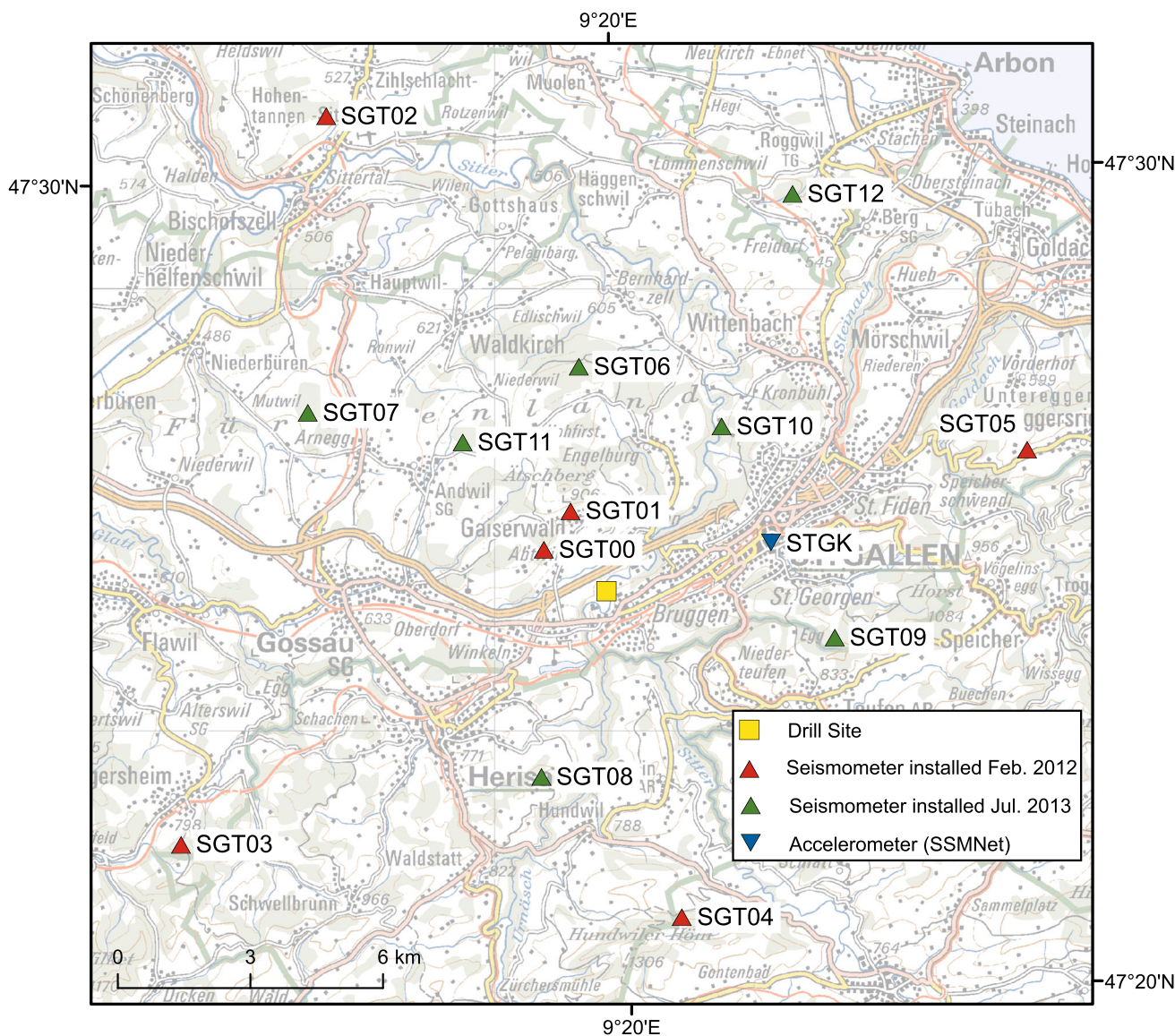


Fig. 2 Station array for monitoring seismicity related to the St. Gallen geothermal project in the region of St. Gallen. Red triangles basic monitoring network with on-line data acquisition (see Table 6 in

“Appendix”); green triangles mobile stations (SGT06-09: stations with on-line data acquisition, SGT10-12: stations without on-line data acquisition). The yellow square shows the location of the drill site

seismic networks, a high-gain predominantly broad-band seismometer network (Table 4 in “Appendix”) and a low-gain accelerograph network (Table 5 in “Appendix”). The former is designed to continuously monitor ongoing earthquake activity down to magnitudes well below the human perception threshold, whereas the latter is principally aimed at engineering concerns and thus focuses on recording ‘strong motions’ in urban areas. In addition, the SED operates a number of temporary stations for various projects (Table 6 in “Appendix”). SED stations with on-line data acquisition that were operational at the end of 2013 are shown in Fig. 1.

The ongoing densification of the Strong Motion accelerograph network with real-time continuous very-broadband accelerometers (Clinton et al. 2011; Cauzzi and Clinton 2013) continued. In 2013, eight new stations were installed (SBAW, SRHE, SLOP, SBAJ2, SRHH, SBERN, SBAV, SBAM2), which concludes the 30-station 4-year first phase of the two-phase project (Michel et al. 2014). Six of these stations have been installed in the city of Basel through a research project with the canton. Due to construction works, the broadband station at EMV (Emosson Dam) was dismantled in 2012. In

2013, a strong motion station SEMOS was installed near the original site of EMV.

The earthquakes induced by the geothermal project in Basel in 2006 have raised concerns about potential seismicity induced by other geothermal projects (even those that do not involve the enhancement of permeability through massive water injections). It is now common practice for responsible operators to include local monitoring capabilities for such projects. An array to monitor a geothermal experiment during the summer of 2013 near St. Gallen that was installed in 2012 was monitored throughout 2013, with some densification following the induced sequence (Fig. 2). This network was operated in cooperation with the St. Galler Stadtwerke and the Swiss Federal Office of Energy. In this network station SGT00 includes a borehole short period sensor at 205 m depth and a surface accelerometer located beside the drill site. Five additional surface broadband stations (SGT01, SGT02, SGT03, SGT04 and SGT05) were operated within a 10 km radius around the borehole landing point (Fig. 2). The four-station short period array around the southeast tip of Lake Geneva, associated to a project near Noville to drill for natural gas, was dismantled in the first half of 2013.

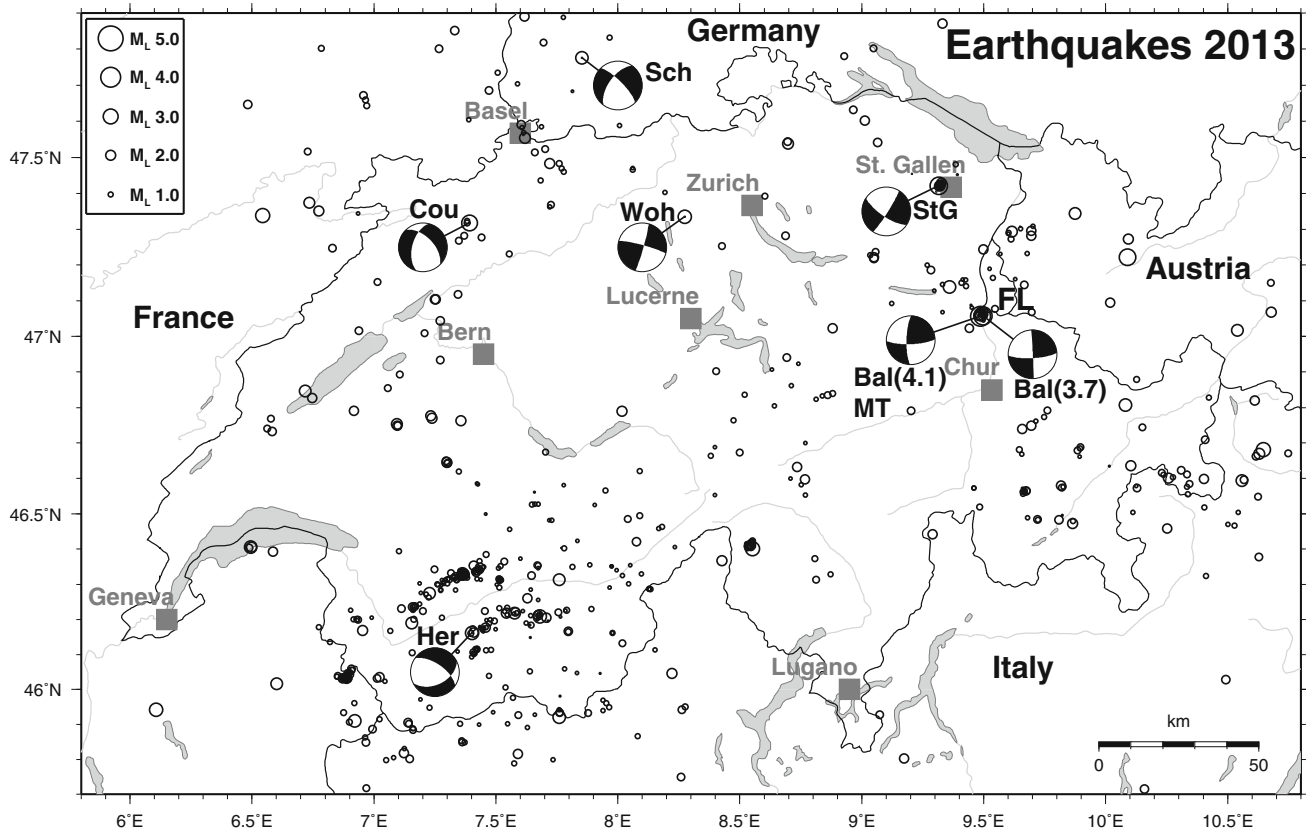


Fig. 3 Epicentres and focal mechanisms of earthquakes recorded by the Swiss Seismological Service during 2013. Epicentres of events mentioned in the text are Balzers (Bal), Courrendlin (Cou),

Hérémece (Her), Schönau (Sch), St. Gallen (StG), Wohlen (Woh). FL marks the territory of Liechtenstein

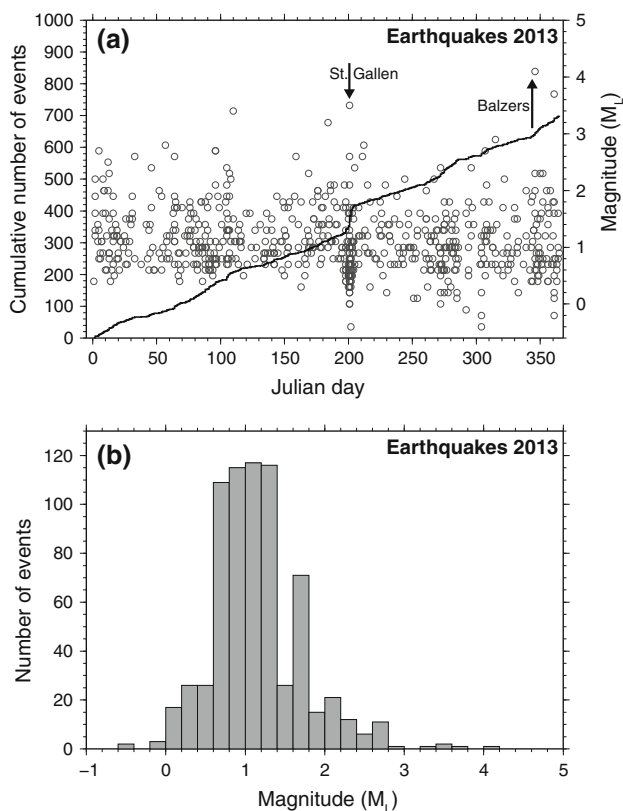


Fig. 4 Earthquake activity during 2013: **a** magnitude of each event and cumulative number of events (arrows mark the M_L 3.5 St. Gallen and M_L 4.1 Balzers event); **b** histogram of magnitudes

In 2013 the construction of a seismic network that monitors the long-term seismicity down to magnitude M_L 1.0 across north-eastern Switzerland was completed. This project, which began in 2011 under a contract with the National Cooperative for the Disposal of Radioactive Waste (Nagra), will improve the understanding of seismotectonic processes in the vicinity of proposed sites for deep nuclear waste repositories. In order to reach this goal, the existing network in northern Switzerland and southern Germany has been significantly densified with seven surface stations and three short-period borehole stations at depths of 100–200 m. These new stations will be in operation for a minimum of 10 years. In 2013, surface stations were installed at EMING, METMA and WALHA (all in Germany) and at DAGMA and ROTHE. Short period borehole sensors were installed at BOBI (154 m) and HAMIK (140 m), both with a surface accelerometer (Fig. 1).

To improve the reliability of locations for events at the periphery of or outside of Switzerland, the SED continues to be engaged in an ongoing cross-frontier cooperative effort to exchange seismic data in real-time. The SED continuously records and archives signals from stations in Austria operated by the *Zentralanstalt für Meteorologie*

und Geodynamik in Vienna (ZAMG, 2 stations); in Italy operated by the *Istituto Nazionale di Geofisica e Vulcanologia* in Rome (INGV, 11 stations), the *Istituto di Geofisica, Università di Genova* (6 stations), the *Zivilschutz der Autonomen Provinz Bozen-Südtirol* (6 stations) and the *Istituto Nazionale di Oceanografia e di Geofisica Sperimentale* (OGS) in Trieste (2 stations); in Germany operated by the *Landeserdbendienst Baden-Württemberg* in Freiburg (LED, 3 stations) and the *Bundesanstalt für Geowissenschaften und Rohstoffe in Hannover* (BGR, 2 stations); and in France by the *Réseau Sismologique et Géodésique Français* (RESIF, 8 stations—3 strong motion). A total of 40 foreign stations were monitored at the SED in 2013, and the number continues to increase as new high-quality stations come on-line in the border region.

2.2 Hypocentre location, magnitude, focal mechanisms and monitoring software

Since 2005, hypocentre locations of the majority local earthquakes have been determined using the software package NonLinLoc (Lomax et al. 2000). The P-wave velocity model used was derived from a 3D tomographic inversion of local earthquake data with constraints from controlled source seismics (Husen et al. 2003), and the S-velocities are calculated from the P-velocity using a V_p/V_s ratio of 1.71. Since October 2012, the Seismic Network uses the SeisComP3 monitoring software for automatic event detection and characterization as well as manual review. More details on the SeisComP3 implementation are in the 2012 Annual Report.

Local magnitudes (M_L) are calculated from the maximum amplitude of the horizontal components of the digital broad-band seismograms filtered to simulate the response of a Wood-Anderson seismograph. The attenuation with epicentral distance is accounted for by an empirically determined relation (Kradolfer and Mayer-Rosa 1988). The final magnitude corresponds to the median value of all on-scale station magnitudes, with stations within 15 km being neglected if possible. For the stronger events, the traditional determination of focal mechanisms from the azimuthal distribution of first-motion polarities (fault-plane solutions) is complemented by moment tensors based on full-waveform inversion. This procedure, based on a time domain inversion scheme developed by Dreger (2003), also provides a moment magnitude, M_W , the best fitting double couple, and an optimal depth estimate based on the given location. An additional procedure has been implemented that routinely and automatically provides estimates of M_W , including earthquakes of lower magnitudes. M_W values are computed using a spectral fitting technique following the method of Edwards et al. (2010).

Table 1 Earthquakes with $M_L \geq 2.5$

Date and time UTC	Lat. (°N)	Lon. (°E)	X/Y (km)	Z (km)	Mag. (M_L)	Mag. (M_W)	Mag. ($M_{WSP\text{EC}}$)	Q	Location
2013/01/05 07:46:51	46.209	7.679	618/117	4	2.7	–	2.7	A	Pte. Tourtemagne, VS
2013/01/12 22:24:12	46.406	6.495	527/140	8	2.5	–	2.7	B	Thonon-les-Bains, F
2013/02/02 06:16:59	45.922	7.760	625/86	2	2.6	–	2.7	B	Breithorn, I
2013/02/26 11:57:20	46.401	8.551	685/139	8	2.8	–	2.6	A	Val Bavona, TI
2013/03/05 01:17:42	47.139	9.360	746/223	3	2.6	–	2.8	B	Walenstadt, SG
2013/04/06 20:49:06	45.943	6.107	497/89	3	2.7	–	3.0	B	Annecy, F
2013/04/06 23:15:29	46.162	7.402	597/112	7	2.7	–	2.7	A	Hérémece, VS
2013/04/20 12:21:33	47.222	10.090	801/233	4	3.4	–	3.5	B	Lech, A
2013/06/08 03:06:05	47.776	7.853	631/292	23	2.6	–	2.4	A	Schönau i. Schwarzwald, D
2013/07/03 14:13:50	47.318	7.391	596/241	25	3.2	–	3.0	A	Courrendlin, JU
2013/07/20 03:30:55	47.421	9.316	742/254	4	3.5	3.3	3.5	A	St. Gallen, SG
2013/07/20 19:50:27	46.808	10.081	802/187	7	2.6	–	2.7	B	Val Lavinuoz, GR
2013/07/30 01:58:33	45.911	6.921	560/84	6	2.6	–	2.8	B	Chamonix, F
2013/07/31 09:31:09	46.682	10.646	845/175	10	2.8	–	2.9	A	Schluderns, I
2013/11/03 21:42:44	47.335	8.274	663/243	30	2.7	–	2.4	A	Wohlen, AG
2013/11/11 20:22:25	47.339	6.544	532/243	3	2.9	–	3.0	B	Chazot, F
2013/12/12 00:59:19	47.058	9.491	756/214	6	4.1	3.7	3.7	B	Balzers, FL
2013/12/27 07:08:28	47.058	9.496	756/214	6	3.7	–	3.4	A	Balzers, FL

The values listed under M_W are moment magnitudes derived from the moment tensor inversion shown in Fig. 6. The values listed under $M_{WSP\text{EC}}$ are the moment magnitudes calculated from the spectral fitting method documented in Edwards et al. (2010). The quality rating (Q) is defined in Table 2

Table 2 Criteria and location uncertainty corresponding to the quality rating (Q) of the hypocentral parameters in the event list in Table 1

Rating	Criteria		Uncertainty	
	GAP (°)	DM (km)	H (km)	Z (km)
A	≤ 180	$\leq 1.5 \times Z$	≤ 2	≤ 3
B	≤ 200	≤ 25	≤ 5	≤ 10
C	≤ 270	≤ 60	≤ 10	> 10
D	> 270	> 60	> 10	> 10

GAP largest angle between epicentre and two adjacent stations, DM minimum epicentral distance, H horizontal location, Z focal depth

3 Seismic activity during 2013

3.1 Overview

During 2013, the Swiss Seismological Service detected and located 699 earthquakes in the region shown in Fig. 3. Based on criteria such as the time of occurrence, the location, and signal character or on direct communication, 208 additional seismic events were identified as quarry blasts. Magnitude values of the events recorded in 2013 range from M_L -0.4 to 4.1 (Fig. 4). The events with $M_L \geq 2.5$ and the criteria used to assign the quality rating for the given locations as well as the corresponding

estimated location accuracy are listed in Tables 1 and 2. Table 1 also includes the available M_W values derived from the spectral fitting method of Edwards et al. (2010) and from method of Dreger (2003) when available. Fault-plane solutions based on first-motion polarities are shown in Figs. 5 and 6 (see also Fig. 3) and their parameters are listed in Table 3.

Figure 7 shows the epicentres of the 911 earthquakes with $M_L \geq 2.5$, which have been recorded in Switzerland and surrounding regions over the period 1975–2013. These events represent about 8 % of the total number of events detected during that time period in the same area. The chosen magnitude threshold of M_L 2.5 ensures that the data set is complete for the given period (Nanjo et al. 2010) and that the number of unidentified quarry blasts and of mis-located epicentres is negligible.

3.2 Significant earthquakes of 2013

3.2.1 Hérémece

Although the magnitude reached only M_L 2.7, the event at Hérémece, which occurred on April 6th at 23:15 UTC, was felt by many people in the Rhone Valley and south of it. About 150 felt reports were collected and the maximum observed intensity was IV. The focal depth of 7 km is well

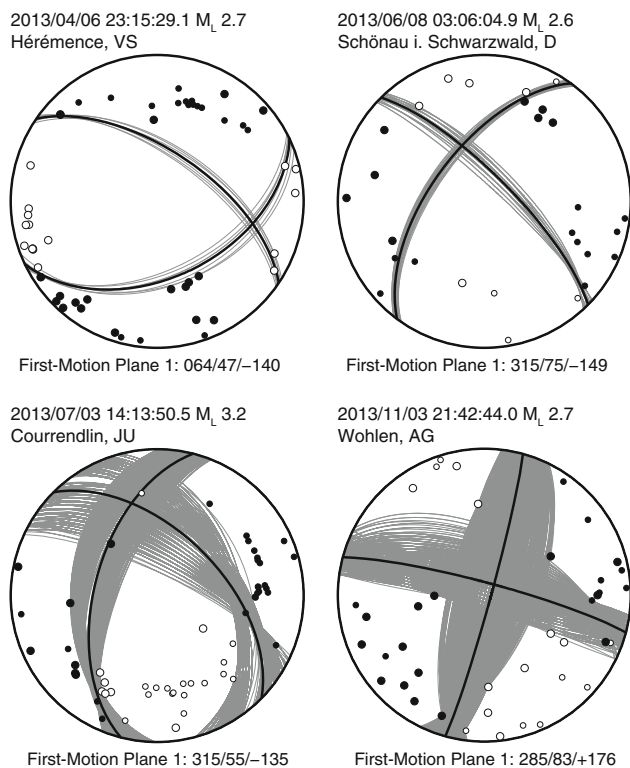


Fig. 5 Fault-plane solutions based on first-motion polarities for four events in 2013 (Hérémence, Schönau, Courrendlin, Wohlen; see Table 3). All stereograms are lower hemisphere, equal-area projections. *Solid circles* correspond to compressive first motion (*up*); empty circles correspond to dilatational first motion (*down*). The take-off angles were computed with the NonLinLoc software (Lomax et al. 2000), using the 3D velocity model of Husen et al. (2003). *Grey lines* show sets of acceptable solutions derived by the HASH algorithm (Hardebeck and Shearer 2002); *black bold lines* indicate the (preferred) average focal mechanisms of all accepted solutions

constrained by several stations at about 8 km epicentral distance and consistent with a source in the upper Penninic Nappes. The focal mechanism shown in Fig. 5 (see also Fig. 3) is well constrained by first motion polarities of P-phases and indicates an extensional regime in agreement with other focal mechanisms south of the Rhone Valley (e.g. Kastrup et al. 2004).

3.2.2 Schönau

The small event of M_L 2.6 that occurred on June 8th near Schönau in Germany (Fig. 3) is another example of a lower-crustal earthquake in 2013. Its focal depth of 23 km is well constrained. The station BFO of the Black Forest Observatory in Schiltach, Germany, was included to improve the azimuthal coverage of the location and the focal mechanism. Because station BFO is not included in the routinely used model of Husen et al. (2003), the earthquake was located in the regional 3D model of Diehl

et al. (2009). Although the earthquake is located outside of Switzerland, the distribution of first motion polarities constrains the focal mechanism reasonably well (Fig. 5). It is mainly a strike-slip mechanism with an almost E–W oriented T-axis (Table 3) and therefore typical for lower-crustal earthquakes in this region (e.g. Kastrup et al. 2004; Singer et al. 2014).

3.2.3 Courrendlin

The M_L 3.2 earthquake of July 3rd with epicentre at Courrendlin (Fig. 3) occurred at a depth of 25 km in the lower crust beneath the Swiss Jura. It was felt by only few people in the region. Although strike and dip of the focal mechanism have large uncertainties, the distribution of first-motion polarities indicates a normal fault mechanism with a strike-slip component (Fig. 5) and orientations of P and T-axes consistent with other mechanisms in the region (e.g. Kastrup et al. 2004; Singer et al. 2014).

3.2.4 Induced seismicity in St. Gallen

Initiated by the utility company of St. Gallen, the St. Gallen geothermal project was targeting existing fracture zones in the Mesozoic limestone layers of the Molasse sedimentary basin as a reservoir for geothermal energy. The targeted fracture zone, which was assumed to be seismically inactive, was imaged by a 3D seismic survey prior to drilling. Drilling operations were initiated in early 2013 and the target depth of 3,660 m (bls) was reached in early July 2013. Starting in July 2012 a dense monitoring network was installed by the SED (for detailed description of the SGT-network, see Sect. 2.1; Figs. 1 and 2) with the goal to provide fast information on potentially induced seismicity to the operator and the public. In parallel to the national detection pipeline, a special processing pipeline was setup in the SeisComp3 monitoring system, including all on-line SGT stations plus selected national high-gain stations in the region. The national as well as SGT processing pipelines were used for automatic triggering, locating, and alarming of potentially induced seismicity. STA/LTA triggers at six stations were required to generate an automatic location in the SeisComp3 system. To further lower the detection threshold, an additional semi-automated screening of signals was performed. In Figs. 4 and 8 we included only events originally detected by one of the automatic SeisComp3 pipelines.

Seismicity initiated shortly after the first injection test was carried out on July 14th (Fig. 8). The following increase in the seismicity coincides with acid stimulations on July 17th. Starting around noon on July 19th, methane entered the borehole. During the following ‘well control’ sequence, the operators decided to pump cold water into

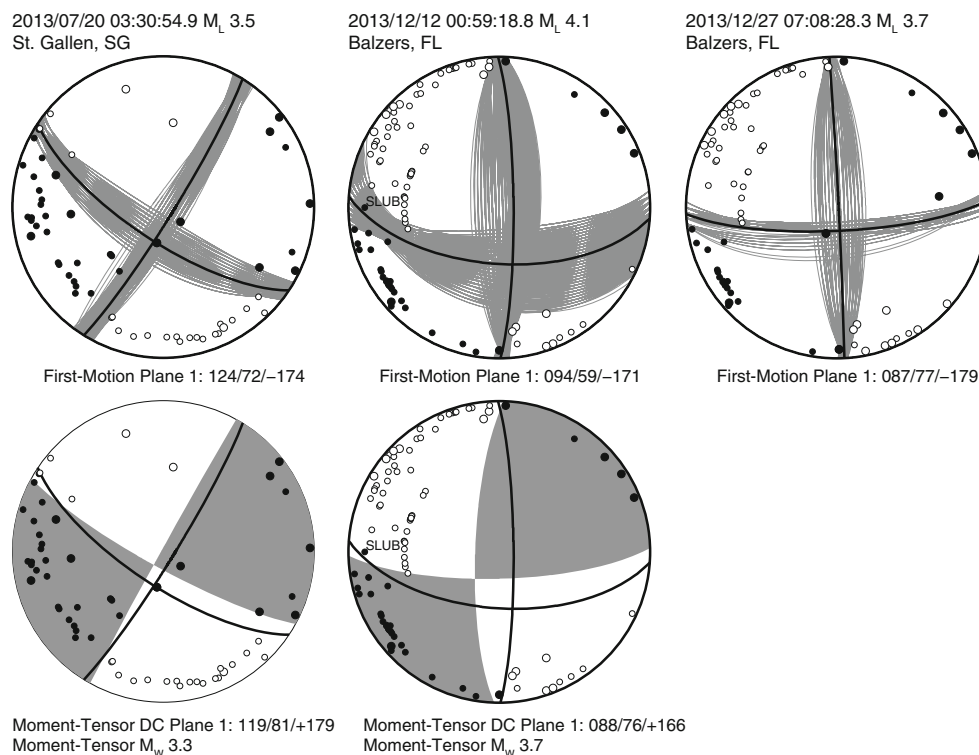


Fig. 6 Fault-plane solutions based on first-motion polarities for three events in 2013 (*upper row* St. Gallen, Baltzers M_L 4.1 mainshock, and Baltzers M_L 3.7 aftershock; see Table 3). *Symbols* and explanation as in Fig. 5. For two of these events (*lower row*), the double-couple part

of the full waveform moment tensor solution is shown as a beach-ball symbol (St. Gallen, Baltzers mainshock—items marked MT in Table 3). *Black bold lines* indicate the preferred first-motion solution of the same event

Table 3 Focal mechanism parameters based on first-motion polarities and full moment tensor inversions (marked as MT) of 7 earthquakes in 2013 (see Figs. 5 and 6)

Location	Date and time UTC	Depth (km)	Mag.	Plane 1 Strike/Dip/Rake	Plane 2 Strike/Dip/Rake	P-axis Azimuth/Plunge	T-axis Azimuth/Plunge
Hérévence	2013/04/06 23:15:29	7	2.7	064/47/−140	304/62/−51	265/55	7/9
Schönau	2013/06/08 03:06:05	23	2.6	315/75/−149	216/60/−17	179/32	83/10
Courendlin	2013/07/03 14:13:50	25	3.2	315/55/−135	195/55/−45	165/55	255/0
St. Gallen	2013/07/20 03:30:55	4	3.5	124/72/−174	32/84/−18	347/17	79/8
St. Gallen-MT		5	3.3	119/81/179	209/89/9	344/6	74/7
Wohlen	2013/11/03 21:42:44	30	2.7	285/83/176	15/86/7	150/2	240/8
Baltzers	2013/12/12 00:59:19	6	4.1	094/59/−171	359/82/−31	312/27	51/16
Baltzers-MT		5	3.7	088/76/166	181/76/14	315/0	45/20
Baltzers	2013/12/27 07:08:28	6	3.7	087/77/−179	357/89/−13	311/10	43/8

the well in order to reduce the pressure buildup. At 7 p.m. local time on July 19th seismicity started to increase with a magnitude M_L 2.1 event at 2:40 a.m. local time on July 20th. At 5:30 a.m. local time, the largest event of the sequence occurred, with a magnitude of M_L 3.5 (M_W 3.3). The M_L 3.5 earthquake was followed by several ‘aftershocks’ and the seismicity finally ceased with the end of well-control phase on July 25th (Fig. 8). The increase in

seismic activity starting in mid September coincides with well cleaning activities. Once production tests started on October 15, seismicity essentially stopped (Fig. 8). In total 105 events with magnitudes between M_L −0.4 and 3.5 have been detected with the automatic system (Fig. 8). It should be noticed, however, that the routinely determined local magnitudes of small events in Fig. 8 are overestimated.

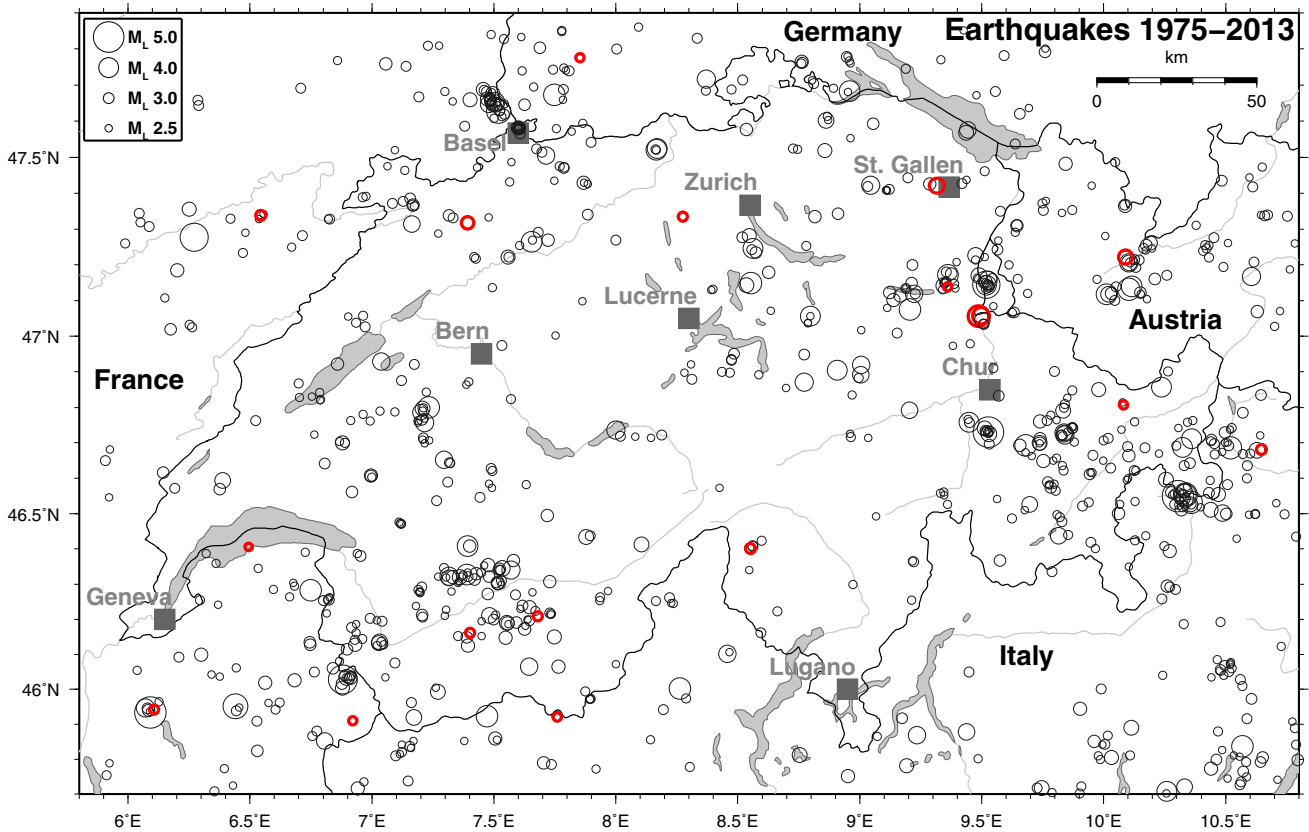


Fig. 7 Epicentres of earthquakes with magnitudes $M_L \geq 2.5$, during the period 1975–2013. Grey circles denote earthquakes in the period 1975–2012, bold red circles indicate earthquakes in 2013

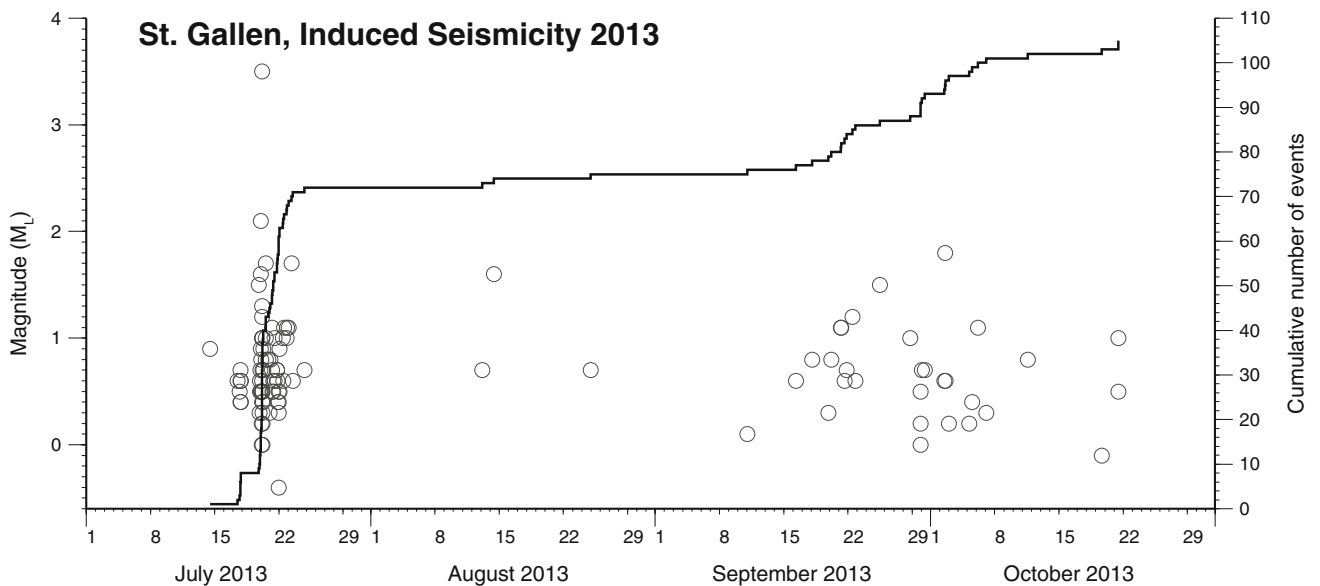


Fig. 8 Cumulative number of events and magnitude of the induced earthquakes in St. Gallen as detected by STA/LTA trigger algorithms using on-line stations of the St. Gallen network (Fig. 2)

complemented by stations of the national high-gain network in the region. The routinely derived network M_L is overestimated in cases where magnitudes are determined from local SGT stations alone

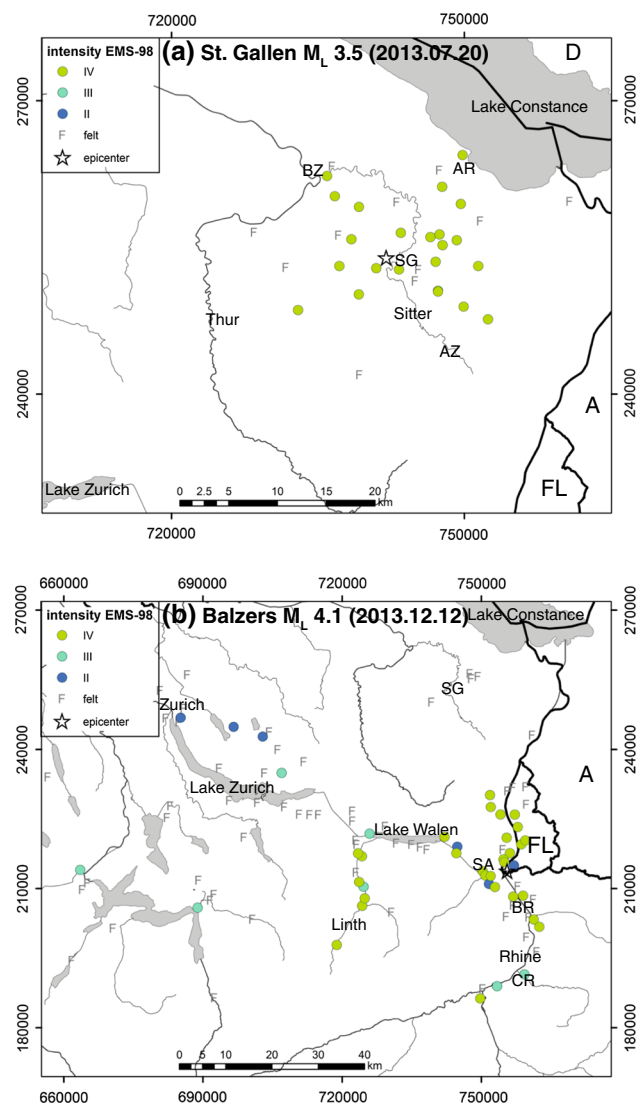


Fig. 9 Macroseismic intensities (EMS-98) of (a) the M_L 3.5 St. Gallen event of July 20 and (b) the M_L 4.1 Balzers mainshock of December 12. Stars indicate the epicentres of the events. Geographic labels: A Austria, D Germany, FL Liechtenstein, AR Arbon, AZ Appenzell, BR Bad Ragaz, BZ Bischofszell, CR Chur, SA Sargans, SG St. Gallen

Macroseismic intensities of the M_L 3.5 event reached degree IV on the European Macroseismic Scale EMS-98 (Fig. 9a). Compared to the induced event of Basel in 2006 the intensities reported for the St. Gallen event are typically one degree lower (Intensity IV vs. V) and the felt radius is smaller (e.g. Baer et al. 2007), even though it had a similar magnitude. The focal depth of the M_L 3.5 event is about 4 km using Pg and Sg phases at distances <80 km in combination with the velocity model of Husen et al. (2003). The resolution of the routinely determined focal depth does not allow deciding whether the source is within the Mesozoic sediments or in the basement. First results of a more detailed analysis that is still underway indicate that

the majority of events are located in the Mesozoic sediments. A moment tensor (MT) solution is available for the M_L 3.5 event (Fig. 6), which indicates almost pure strike-slip motion. The MT is confirmed by the solution derived from the analysis of first-motion polarities (Fig. 6; see also Fig. 3). Nodal planes of both solutions agree very well. Preliminary results of a relative relocation study show that the left-lateral, NE–SW striking plane was the active plane.

3.2.5 Wohlen

Another lower crustal earthquake of M_L 2.7 occurred on November 3rd near Wohlen (Fig. 3). It was felt by a few individuals in the canton Aargau. The well-constrained depth derived by the routine location procedure is 30 km and therefore only about 2 km above the Moho at this location (Wagner et al. 2012). Although gaps in the azimuthal distribution of first-motions polarities lead to larger uncertainties of the computed nodal planes (Fig. 5), the solution is consistent with a strike-slip mechanism with an orientation typical for lower crustal earthquakes in this region (e.g. Kastrup et al. 2004; Singer et al. 2014).

3.2.6 Balzers

On December 12th an earthquake with an M_L of 4.1 (M_W 3.7) was located in the Rhine valley, close to the village of Balzers in southern Liechtenstein (Fig. 3). The M_L 4.1 mainshock occurred at 00:59 a.m. UTC and was widely felt in the Alpine Rhine valley from Chur towards Lake Constance, throughout Liechtenstein and in adjacent areas of Switzerland and Austria (Fig. 9b). The event was strong enough to awaken a considerable portion of the population, and let suspended objects swing, china clatter, doors rattle, etc. More than 750 felt reports have been collected, but no confirmed damage to buildings or objects has been reported. The analyzed felt reports suggest an intensity of IV on the EMS-98 macroseismic intensity scale. Intensities of grade IV reported in the Linth valley in the canton Glarus (Fig. 9b) are presumably due to site effects.

Peak ground acceleration (PGA) reached maximum values of about 3 % g at the closest station to the epicentre, while the maximum recorded peak ground velocity (PGV) was about 0.4 cm s^{-1} . The real-time strong-motion stations closest to the epicentre were three stations in the area of Buchs, SG, characterized by different site conditions. SBUB is located on hard rock on the Buchserberg, SBUA2 is located on the Altendorf alluvial fan bordering the Rhine basin, while SBUH is located in the center of the deep Rhine basin in Buchs. Figure 10a shows the acceleration seismograms of the M_L 4.1 mainshock recorded at the three stations. The amplitude of the signal is larger for the stations on sediments (SBUH, SBUA2) compared to the hard

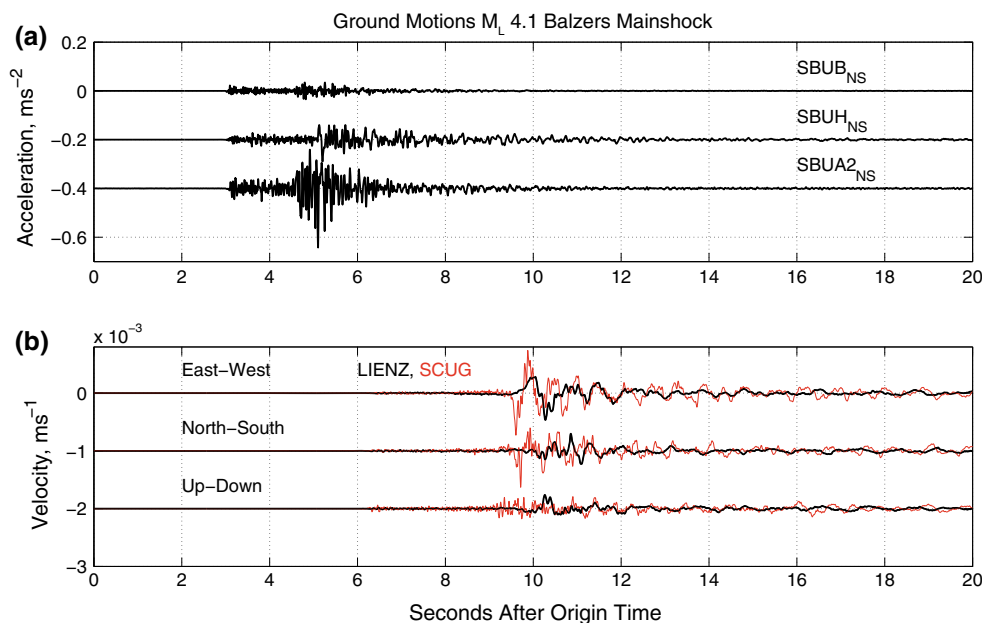


Fig. 10 Ground motions records of the M_L 4.1 Balzers mainshock of December 12th (a) Restituted acceleration seismograms recorded at the national strong-motion stations SBUB, SBUH, and SBUA2 (NS-component, 11–13 km epicentral distance). Signals are filtered with a 0.33–100 Hz, 4th order, Butterworth band-pass filter. Seismograms of station SBUH and SBUA2 were offset by -0.2 and -0.4 ms^{-2} , respectively. Note the larger amplitude at stations on sediments (SBUH, SBUA2) compared to the hard rock site (SBUB). **b** Velocity

seismograms obtained after integration of the acceleration recording at station LIENZ (*black*; at 26 km distance) and SCUG (*red* at 23 km distance). Restitution to ground acceleration and band-pass filtering (0.33–100 Hz, 4th order, Butterworth) was applied before integration. North–South and Up–Down channels were offset by -0.001 and -0.002 ms^{-1} , respectively. Note the relatively long-period waves starting at about 10–11 s after origin time at station SCUG, which are associated to the basin response

rock site (SBUB). Site effects associated to basin response were also observed at the strong-motion station SCUG, installed in the Rhine basin in Chur. The response of the sedimentary basin is particularly apparent after integration of the acceleration waveforms to velocity, as shown in Fig. 10b. While the amplification of velocity values with respect to a rock site at comparable distance is moderate (LIENZ, Fig. 10b), the time histories at the two sites exhibit remarkable differences. At SCUG, the onset of relatively long-period waves of 0.5 s associated to the basin response (Michel et al. 2014) can be clearly appreciated in the horizontal components of ground-motions starting at about 10–11 s after origin. The duration of significant shaking at SCUG is significantly larger than at the rock site LIENZ, where only a few dominant cycles of ground motion can be read from the velocity traces (Fig. 10b).

The M_L 4.1 mainshock was followed by a sequence of aftershocks with local magnitudes of locatable events ranging between M_L -0.2 and 3.7. The largest M_L 3.7 aftershock occurred on December 27th at 07:08 a.m. UTC and the aftershock seismicity finally ceased after mid March 2014. At the time of the M_L 4.1 mainshock, the closest station of the SDSNet, PLONS, was not

operational. The closest station was SBUB (Fig. 1) at a distance of about 11 km. Using all 143 manually picked first arriving Pg, Sg, and Pn phases results in a focal depth of about 4 ± 1 km. Using only Pg and Sg phase at distances <150 km results in a focal depth of 6 ± 1 km. The focal depth of 4 km seems mainly constrained by P phases at epicentral distances >150 km. Given the uncertainties in the computation of Pg and Pn ray paths and travel times for these distances (e.g. Diehl et al. 2013), the derived uncertainty of ± 1 km might underestimate the true error of the absolute focal depth and the source of 6 km derived from the subset of picks is as plausible as the 4 km source.

To better constrain the focal depth of the aftershocks, a temporary seismic station (QSA01) was installed on the castle hill in Balzers in a distance of about 1 km from the mainshock on December 13th. At the same time the permanent station PLONS was again brought online. With the two additional near-by stations, the uncertainty of the focal depth of the M_L 3.7 aftershock is reduced. The solution derived from all 120 first arriving P and S phases results in a focal depth of 6 ± 0.5 km. The imperfect knowledge of the velocity structure, especially at the closest stations (i.e. QSA01), might have a strong impact on the absolute focal depth. The top of the crystalline basement in this area is at

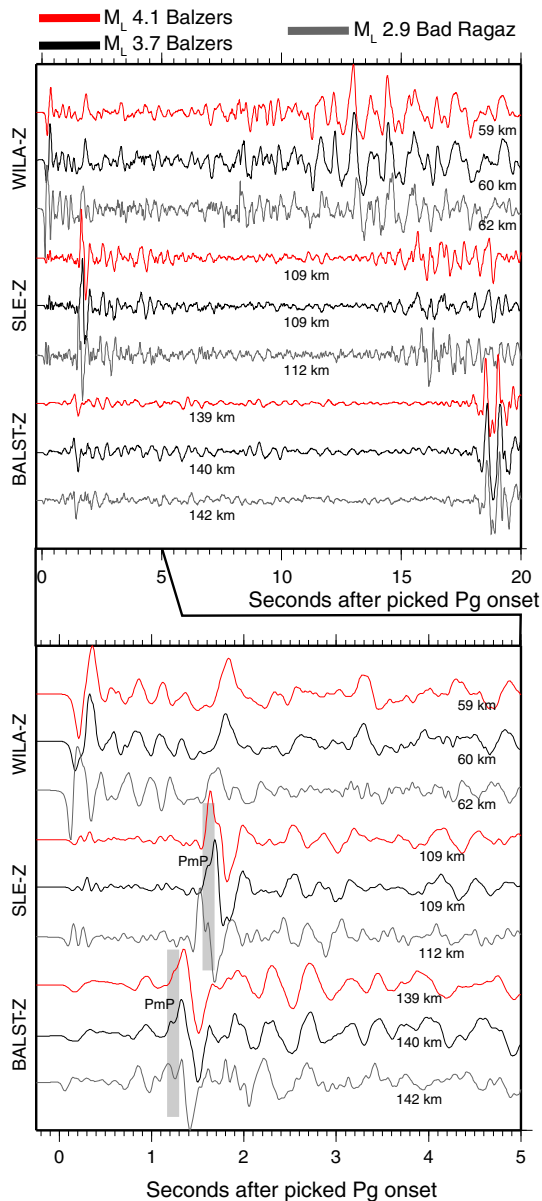


Fig. 11 Displacement seismograms of the M_L 4.1 Balzers mainshock (red), the M_L 3.7 Balzers aftershock (black), and the M_L 2.9 Bad Ragaz event of 2005 (grey) recorded on vertical components at the national high-gain stations WILA, SLE, BALST (see Fig. 1). The signals are filtered with a 1–30 Hz, 2nd order, Butterworth band-pass filter. The time window in the upper panel includes P and S waves, the time window in the lower panel is focused on the P wave. Numbers next to the seismograms indicate the epicentral distance. The high degree in similarity between the M_L 4.1 mainshock and the M_L 3.7 aftershock, especially the S–P and PmP–Pg times, suggests that both events have similar source locations and focal mechanisms. The general similarity with the Bad Ragaz event suggests a similar source region for both sequences

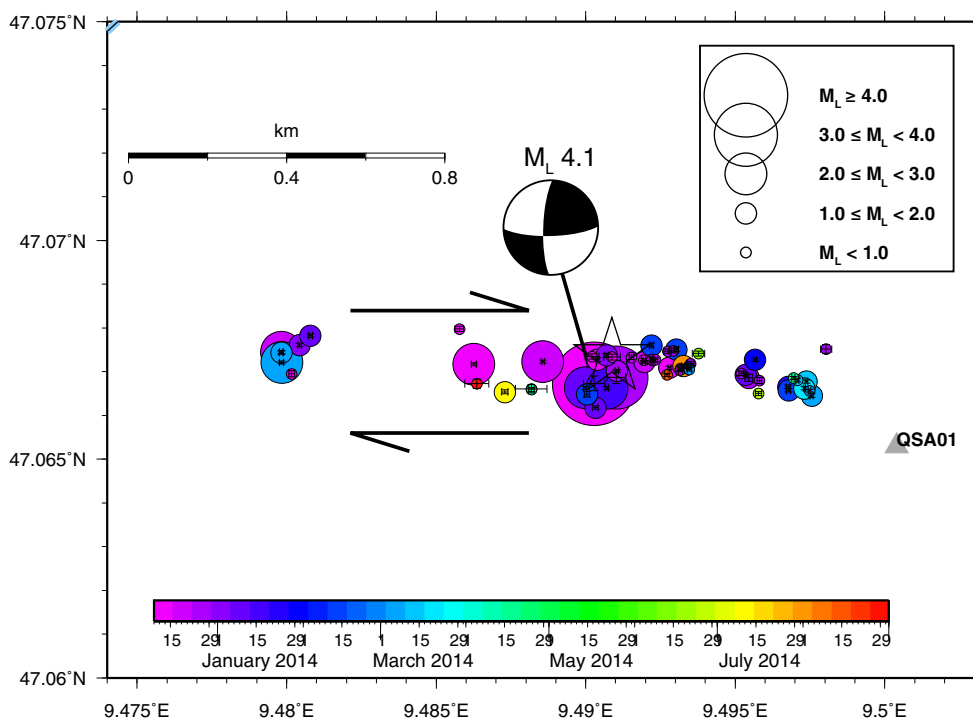
a depth of about 6 km and it is overlain by a thick and complex sedimentary sequence (Pfiffner and Hitz 1997). Overestimating the velocities of the sedimentary sequence at QSA01 would result in an overestimated focal depth. Assuming an average P-wave velocity of 5.0–5.3 km/s for

the medium above the hypocentre (e.g. Ye et al. 1995) and a V_p/V_s ratio in the range of 1.70–1.8, the S–P time of 0.9 s measured at station QSA01 for the M_L 3.7 aftershock is consistent with a depth between 5.6 and 6.8 km. Thus the focal depth of 6 ± 0.5 km derived in the 3D model of Husen et al. (2003) is in good agreement with the observed S–P time at QSA01. A depth of 4 km, as derived for the M_L 4.1 mainshock, would require an average $V_p < 5$ km/s, and/or $V_p/V_s > 1.8$. Figure 11 shows a comparison of waveforms of the M_L 4.1 mainshock with the M_L 3.7 aftershock at three stations. The high degree of similarity between the seismograms, especially the S–P and PmP–Pg times, suggests that both events have similar source locations and focal mechanisms. It seems therefore plausible that both events occurred in a depth of about 6 km and we prefer the depth of 6 km derived from the subset of picks as the depth of the mainshock (Table 1).

The remaining uncertainties in the absolute focal depth (at least ± 0.5 km) and in the geological interpretation of the seismic data of Pfiffner and Hitz (1997), however, do not allow deciding whether the earthquakes occurred in the crystalline basement or in the overlying sediments. Between 2000 and 2005 a sequence of earthquakes occurred close to Bad Ragaz, just about 3 km south of the 2013 Balzers sequence. Focal depths reported for these events vary between 7 and 8 km and the impulsive signal character of P and S waves as well as the clear records at large distances have been interpreted as qualitative indications for a source in the crystalline basement (Baer et al. 2001; Deichmann et al. 2006; Marschall et al. 2013). Figure 11 shows a comparison of the two strongest Balzers events with the 2005 M_L 2.9 Bad Ragaz event. The similarity of the general signal character as well as PmP–Pg times suggest a similar source region for both sequences. Both sequences seem to locate in the uppermost part of the basement, but with the given uncertainties a source in the Mesozoic sediments, as discussed for the St. Gallen sequence before, cannot be entirely excluded.

The MT solution derived for the M_L 4.1 mainshock indicates a strike-slip mechanism with practically N–S and E–W striking nodal planes (Figs. 3, 6; Table 3). The solution derived from the analysis of first-motion polarities generally agrees with the MT, but strike and dip of the nodal planes show uncertainties due to gaps in the azimuthal distribution (Fig. 6). The clear upward motion observed at station SLUB (Fig. 1) falls within the extensional part of the MT solution (Fig. 6). This discrepancy is most likely related to a modeling error in the take-off angle calculation. No MT solution was derived for the M_L 3.7 aftershock, but the two additional near-by stations QSA01 and PLONS significantly reduce the uncertainty of the first-motion mechanism (Fig. 6). The solution agrees very well with the MT solution of the mainshock and, in combination

Fig. 12 Relative relocations of the Balzers sequence using double-difference techniques in combination with waveform cross-correlation. The sequence comprises 62 earthquakes recorded between December 9th 2013 and August 25th 2014. Bars indicate relative location errors; colors indicate origin time of the events. The *star* indicates the epicentre of the foreshock of December 9th, 2013. *Grey triangle* shows the location of the temporary seismic station QSA01 installed during the day after the mainshock



with the similarity of waveforms (Fig. 11), suggests an almost identical slip direction.

Both mechanisms are very similar to the two mechanisms derived for the Bad Ragaz events in 2000 and 2005 (Baer et al. 2001; Deichmann et al. 2006). Here, the N–S striking plane with left-lateral motion was identified as the active plane by relative relocations of fore- and aftershocks (Marshall et al. 2013). To resolve the active plane of the Balzers sequence we relocated 62 fore- and aftershocks in the period between December 2013 and August 2014 using double-difference techniques in combination with time-domain waveform cross-correlation (Waldhauser and Ellsworth 2000). The relocated hypocentres form an E–W striking lineament that extends roughly 1.4 km horizontally (Fig. 12) and thus identifying the E–W striking nodal plane with dextral strike-slip motion as the active plane. The strike of the active planes of the Bad Ragaz sequence and the Balzers sequence are almost perpendicular to each other and it is therefore implausible that the two sequences are the expression of one major N–S striking fault in the Rhine valley.

3.2.7 Seismicity associated with the former deep heat mining project in Basel

The seismic activity induced by the geothermal project in Basel in 2006 and 2007 (e.g. Deichmann and Ernst 2009; Deichmann and Giardini 2009) continued to decrease over the years 2008–2011, with only one event (M_L 0.6) being

recorded by the national network in 2010. In 2012 activity seemed to have picked up again: five events, with magnitudes between $M_L = 0.9$ – 1.2 , were associated with the stimulated rock volume (Diehl et al. 2013). Master-event relocation confirmed that in 2013 two events (on June 29th and December 28th) occurred at the southern edge of the activated rock volume (Deichmann et al. 2014). The M_L 0.8 event of December 2013 occurred within about 100 m of the three events recorded in December 2012, whereas the hypocenter of the M_L 1.7 event of June 29th was about 300 m shallower and about 200 closer to the borehole (Deichmann et al. 2014). However, both events can be regarded as belonging to the sequence that has been active since 2007 and is located above the casing shoe at the southern periphery of the main microseismic cloud.

4 Discussion

In 2013, as in previous years, a large portion of the seismic activity was concentrated in the Valais, Graubünden, and the immediately adjacent regions. Routinely calculated focal depths for all but 23 events recorded in 2013 are <16 km. All but two of the deeper hypocentres occurred below the Molasse Basin and the Jura of northern Switzerland and southern Germany, with the main activity clustered between 7°E and 10°E (e.g. Deichmann 1992; Deichmann et al. 2000a; Singer et al. 2014). The other two events in 2013 occurred at about 20 km depth beneath the

southern margin of the Alps in northern Italy. Both solutions have considerable azimuthal gaps and locations are poorly constrained. The M_L 1.5 event of October 4th, however, locates just 9 km to the southwest of the M_L 3.8 Erba earthquake of 2001, which represents an example for a well-constrained lower crustal earthquake at the southern margin of the Alps in northern Italy (e.g. Deichmann et al. 2002).

Overall, the seismic activity in and around Switzerland, in terms of the number of events, appears exceptionally high in 2013. The 699 located earthquakes in 2013 represent the highest number of earthquakes since the year 2004 (about 670 located earthquakes). The number is partly explained by the two earthquake sequences in St. Gallen and Balzers and removing the 105 induced earthquakes of St. Gallen results in a number closer to the 13-year average of 497 earthquakes per year. The exceptional high number of 208 located quarry blasts (more than twice the 13-year average of 90 blasts per year) might reflect changes in the detection threshold due to network enhancement or, alternatively, changes in the earthquake analysis procedures. The total number of 18 events with $M_L \geq 2.5$, on the other hand, is still slightly below the yearly average of about 23 events over the previous 38 years in this magnitude range.

Acknowledgments Monitoring the seismicity in a small country is not possible without international cooperation. Automatic data exchange in real-time has been implemented with Austria operated by the *Zentralanstalt für Meteorologie und Geodynamik* in Vienna (ZAMG); with Italy operated by the *Istituto Nazionale di Geofisica e Vulcanologia* in Rome (INGV), the *Istituto di Geofisica, Università di Genova*, the *Zivilschutz der Autonomen Provinz Bozen-Südtirol* and the *Istituto Nazionale di Oceanografia e di Geofisica Sperimentale* (OGS) in Trieste; with Germany operated by the *Landeserdbeben dienst Baden-Württemberg* in Freiburg (LED) and the *Bundesanstalt für Geowissenschaften und Rohstoffe* in Hannover (BGR); and with France operated by the *Réseau Sismologique et Géodésique Français* (RESIF). We thank all these institutions for good cooperation. We are also very grateful to our colleagues in the SED seismic network and electronics lab for their relentless efforts in ensuring the continuous reliability of the data acquisition systems and the earthquake monitoring software, and to E. Läderach, S. Brühwiler, and A. Blanchard for administrative and logistic support. We thank M. Schnellmann and H. Müller from Nagra for their support and efforts in installing the NAGRA stations; and G. Siddiqi (BFE) and M. Sonderegger (St. Galler Stadtwerke) for their support for the St. Gallen seismic monitoring project. Financial support from the Nationale Genossenschaft für die Lagerung radioaktiver Abfälle (Nagra) for the operation of several stations in northern Switzerland is gratefully acknowledged. We thank the Swiss Federal Office of Energy for the financial support of project GeoBest (<http://www.seismo.ethz.ch/research/groups/spec/projects/ProjectGeoBest>) that provided the seismic instrumentation for the monitoring network in St. Gallen. St. Galler Stadtwerke are gratefully acknowledged for their financial and logistic support in providing the technical infrastructure for the St. Gallen Network. Financial support for operating seismic stations in the Basel region was given by the Kanton Basel Stadt. We thank N. Deichmann for his advice and support, which helped to improve this report and A. G. Milnes and A. Hirt for their constructive and helpful reviews.

Appendix

List of SED stations with online data acquisition that were operational at the end of 2013 (see Fig. 1).

See Appendix Tables 4, 5 and 6.

Table 4 List of SED stations with online data acquisition that were operational at the end of 2013 (see Fig. 1)

Code	Station name	Type
<i>National on-line network recorded in Zürich</i>		
ACB	Acheberg, AG	EB
AIGLE	Aigle, VD	BB
BALST	Balsthal, SO	BB
BERNI	Bernina, GR	BB
BNALP	Bannalpsee, NW	BB, SM
BOURR	Bourrignon, JU	BB, SM
BRANT	Les Verrières, NE	BB
DAVOX	Davos, GR	BB
DIX	Grande Dixence, VS	BB, SM
EMBD	Embd, VS	BB
EWZT2	Wetzwil, ZH	SP
FIESA	Fiescheralp, VS	BB
FLACH	Flach, ZH	EB
FUORN	Ofenpass, GR	BB
FUSIO	Fusio, TI	BB, SM
GIMEL	Gimel, VD	BB
GRIMS	Grimsel, BE	BB, SM
GRYON	Gryon, VS	EB
HASLI	Hasliberg, BE	BB
LAUCH	Lauchernalp, VS	BB
LIENZ	Kamor, SG	BB, SM
LKBD	Leukerbad, VS	EB
LKBD2	Leukerbad, VS	SP
LLS	Linth-Limmern, GL	BB, SM
MMK	Mattmark, VS	BB, SM
MUGIO	Muggio, TI	BB
MUO	Muotathal, SZ	BB
NALPS	Val Nalps, GR	BB
PANIX	Pigniu, GR	BB
PLONS	Mels, SG	BB
SALAN	Lac de Salanfe, VS	EB
SENIN	Senin, VS	BB, SM
SIMPL	Simplonpass, VS	BB
SLE	Schleitheim, SH	BB
STEIN	Stein am Rhein, SH	EB
SULZ	Cheisacher, AG	BB, SM
TORNY	Torny, FR	BB
TRULL	Trullikon, ZH	EB
VANNI	Vissoie, VS	BB

Table 4 continued

Code	Station name	Type
VDL	Valle di Lei, GR	BB, SM
WEIN	Weingarten, TG	EB
WILA	Wil, SG	BB
WIMIS	Wimmis, BE	BB
ZUR	Zürich-Degenried, ZH	BB, SM

High-gain seismograph stations of the Swiss national network operational at the end of 2013

Instrument type (all three-component): SP = 1-s, EB = 5-s, BB = broad-band, SM = accelerometer. Signals of LKBD2 are transmitted via analog telemetry

Table 5 Strong-motion stations of the Swiss national network with on-line data acquisition operational at the end of 2013

Code	Station name	Type
<i>On-line strong-motion network</i>		
BIBA	Brigerbad, VS	SM
OTTER	Otterbach, BS	SM
SAIG	Aigle-Rue de la Gare, VD	SM
SALTS	Altdorf-Spital, UR	SM
SARK	Sarnen-Kantonsschule, OW	SM
SAUR	Augst-Römermuseum, AG	SM
SBAF	Basel-Friedhofgasse, BS	SM
SBAJ2	Basel, St. Johann, BS	SM
SBAM2	Basel Münster, BS	SM
SBAP	Basel-PUK, BS	SM
SBAT	Basel-Tropenhause, BS	SM
SBAV	Basel, Vogelsang, BS	SM
SBAW	Basel, Wirtschaftsgym., BS	SM
SBEG	Bettingen-Gewerbehause, BS	SM
SBERN	Bern, kleine Schanze, BE	SM
SBIS2	Binningen, BS	SM
SBRS	Brig-Spital, VS	SM
SBUA2	Buchs Kindergarten, SG	SM
SBUB	Buchserberg Malbun, SG	SM
SBUH	Buchs, Hochschule, SG	SM
SCEL	Celerina, GR	SM
SCHS	Schaffhausen Spital, SH	SM
SCOU	Cournillens, FR	SM
SCUC	Scuol-Clozza, GR	SM
SCUG	Chur Gewerbeschule, GR	SM
SEMOS	Emosson Barrage, Bunker, VS	SM
SEPFL	Lausanne EPFL, VD	SM
SFRA	Frenkendorf, BL	SM
SGEV	Genf Feuerwehr, GE	SM
SGRA	Grächen-Ausblick, VS	SM
SIEB	Sierre-Ecole de Borzuat, VS	SM
SINS	Interlaken-Schloss, BE	SM

Table 5 continued

Code	Station name	Type
SIOM	Sion-Mayennets, VS	SM
SIOO	Sion-Ophtalmologie, VS	SM
SIOV	Sion-Valere, VS	SM
SKAF	Kaiseraugst-Friedhof, AG	SM
SLOP	Locarno, Pompieri, TI	SM
SLTM2	Linthal Matt, GL	SM
SLUB	Luzern Bramberg, LU	SM
SLUW	Luzern Werkhofstr., LU	SM
SMAO	Martigny-Rue d'Octodure, VS	SM
SMUK	Muraz-Kläranlage, VS	SM
SMUR	Muraz-Reservoir, VS	SM
SMZW	Muttentz-Waldhaus, BL	SM
SNIB	Sankt Niklaus, VS	SM
SOLB	Solothurn Schule Bruhl, SO	SM
SOLZ	Solothurn-Zeughausgasse, SO	SM
SRER	Reinach Rainenweg, BL	SM
SRHB	Riehen-Bäumlihof, BS	SM
SRHE	Riehen, Erlensträsschen, BS	SM
SRHH	Riehen, Zur Hoffnung, BS	SM
STAF	Tafers, FR	SM
STGK	St. Gallen-Kloster, SG	SM
STSP	Tschierv, GR	SM
SVAM	Vaz-Muldain, GR	SM
SVIL	Visp-Litternaring, VS	SM
SVIO	Visp-Obere Stapfeng., VS	SM
SVIT	Visp-Terbinerstr., VS	SM
SYVP	Yverdon Rue du Phil, VD	SM
SZER	Zerne, GR	SM
SZUZ	Zürich, Zeughauswiese, ZH	SM

Instrument type (all three-component): SM = accelerometer

Table 6 Local seismic networks with on-line data acquisition operational at the end of 2013

Code	Station name	Type
<i>Basel borehole network</i>		
MATTE	Schützenmatte (553)	SP (4.5 Hz)
OTER1	Otterbach (500)	BB, SM
OTER2	Otterbach (2,740)	SP (4.5 Hz)
<i>St. Gallen network</i>		
SGT00	Sennhüslen (SP at 205)	SP, SM
SGT01	Gaiserwald	BB
SGT02	Zihlschlacht	BB
SGT03	Degersheim	BB
SGT04	Schlatt-Haslen	BB
SGT05	Eggersriet	BB

Table 6 continued

Code	Station name	Type
<i>Nagra network</i>		
BERGE	Lenzkirch, DE	BB
BOBI	Böbikon, AG (SP at 154)	SP (4.5 Hz), SM
DAGMA	Lutertal, Dagmarsellen, LU	BB
EMMET	Emmethof, AG	BB
EMING	Emmingen, DE	BB
HAMIK	Hämikon, Däliklerfeld, LU (SP at 140)	SP (4.5 Hz), SM
METMA	Metma, DE	BB
ROTHE	Rothenfluh, BL	BB
STIEG	Oberembrach-Stiegenhof, ZH (SP at 123)	SP (4.5 Hz), SM
WALHA	Wallhausen, DE	BB

Instrument type (all three-component): SP = 1-s, unless otherwise indicated, BB = broad-band, SM = accelerometer. The numbers in parentheses next to the borehole stations are the sensor depth with respect to ground surface in meters

References

- Baer, M., Deichmann, N., Ballarin Dolfin, D., Bay, F., Delouis, B., Fäh, D., et al. (1999). Earthquakes in Switzerland and surrounding regions during 1998. *Eclogae Geologicae Helvetiae*, 92(2), 265–273.
- Baer, M., Deichmann, N., Braunmiller, J., Ballarin Dolfin, D., Bay, F., Bernardi, F., et al. (2001). Earthquakes in Switzerland and surrounding regions during 2000. *Eclogae Geologicae Helvetiae*, 94(2), 253–264.
- Baer, M., Deichmann, N., Braunmiller, J., Bernardi, F., Cornou, C., Fäh, D., et al. (2003). Earthquakes in Switzerland and surrounding regions during 2002. *Eclogae Geologicae Helvetiae Swiss Journal of Geosciences*, 96(2), 313–324.
- Baer, M., Deichmann, N., Braunmiller, J., Clinton, J., Husen, S., Fäh, D., et al. (2007). Earthquakes in Switzerland and surrounding regions during 2006. *Swiss Journal of Geosciences*, 100(3), 517–528. doi:10.1007/s00015-007-1242-0.
- Baer, M., Deichmann, N., Braunmiller, J., Husen, S., Fäh, D., Giardini, D., et al. (2005). Earthquakes in Switzerland and surrounding regions during 2004. *Eclogae Geologicae Helvetiae Swiss Journal of Geosciences*, 98(3), 407–418. doi:10.1007/s00015-005-1168-3.
- Baer, M., Deichmann, N., Fäh, D., Kradolfer, U., Mayer-Rosa, D., Rüttener, E., et al. (1997). Earthquakes in Switzerland and surrounding regions during 1996. *Eclogae Geologicae Helvetiae*, 90(3), 557–567.
- Cauzzi, C. & Clinton, J. (2013). A high- and low-noise model for high-quality strong-motion accelerometer stations. *Earthquake Spectra*: February 2013, 29(1), pp. 85–102. doi:10.1193/1.4000107.
- Clinton, J., Cauzzi, C., Fäh, D., Michel, C., Zweifel, P., Olivieri, M., Cua, G., Haslinger, F., Giardini, D. (2011). The current state of strong motion monitoring in Switzerland. In Akkar, S., Gülkan, P., and van Eck, T. (Eds.) *Earthquake data in engineering seismology: predictive models, data management and networks (geotechnical, geological and earthquake engineering)*. ISBN 10: 9400701519 | 2011.
- Deichmann, N. (1990). Seismizität der Nordschweiz, 1987–1989, und Auswertung der Erdbebenserien von Günsberg, Läuelfingen und Zeglingen. *Nagra Technischer Bericht, NTB 90-46*, Nagra, Baden.
- Deichmann, N. (1992). Structural and rheological implications of lower-crustal earthquakes below northern Switzerland. *Physics of the Earth and Planetary Interiors*, 69, 270–280.
- Deichmann, N., Baer, M., Ballarin Dolfin, D., Fäh, D., Flück, P., Kastrup, U., et al. (1998). Earthquakes in Switzerland and surrounding regions during 1997. *Eclogae Geologicae Helvetiae*, 91(2), 237–246.
- Deichmann, N., Baer, M., Braunmiller, J., Ballarin Dolfin, D., Bay, F., Bernardi, F., et al. (2002). Earthquakes in Switzerland and surrounding regions during 2001. *Eclogae Geologicae Helvetiae Swiss Journal of Geosciences*, 95(2), 249–261.
- Deichmann, N., Baer, M., Braunmiller, J., Ballarin Dolfin, D., Bay, F., Delouis, B., et al. (2000a). Earthquakes in Switzerland and surrounding regions during 1999. *Eclogae Geologicae Helvetiae*, 93(3), 395–406.
- Deichmann, N., Baer, M., Braunmiller, J., Cornou, C., Fäh, D., Giardini, D., et al. (2004). Earthquakes in Switzerland and surrounding regions during 2003. *Eclogae Geologicae Helvetiae Swiss Journal of Geosciences*, 97(3), 447–458.
- Deichmann, N., Baer, M., Braunmiller, J., Husen, S., Fäh, D., Giardini, D., et al. (2006). Earthquakes in Switzerland and surrounding regions during 2005. *Eclogae Geologicae Helvetiae Swiss Journal of Geosciences*, 99(3), 443–452. doi:10.1007/s00015-006-1201-1.
- Deichmann, N., Baer, M., Clinton, J., Husen, S., Fäh, D., Giardini, D., et al. (2008). Earthquakes in Switzerland and surrounding regions during 2007. *Swiss Journal of Geosciences*, 101(3), 659–667. doi:10.1007/s00015-008-1304-y.
- Deichmann, N., Ballarin Dolfin, D., Kastrup, U. (2000b). Seismizität der Nord- und Zentralschweiz. *Nagra Technischer Bericht, NTB 00-05*, Nagra, Wettingen.
- Deichmann, N., Clinton, J., Husen, S., Edwards, B., Haslinger, F., Fäh, D., et al. (2010). Earthquakes in Switzerland and surrounding regions during 2009. *Swiss Journal of Geosciences*, 103(3), 535–549. doi:10.1007/s00015-010-0039-8.
- Deichmann, N., Clinton, J., Husen, S., Edwards, B., Haslinger, F., Fäh, D., et al. (2011). Earthquakes in Switzerland and surrounding regions during 2010. *Swiss Journal of Geosciences*, 104(3), 537–547. doi:10.1007/s00015-011-0084-y.
- Deichmann, N., Clinton, J., Husen, S., Edwards, B., Haslinger, F., Fäh, D., et al. (2012). Earthquakes in Switzerland and surrounding regions during 2011. *Swiss Journal of Geosciences*, 105, 463–476. doi:10.1007/s00015-012-0116-2.
- Deichmann, N., Clinton, J., Husen, S., Haslinger, F., Fäh, D., Giardini, D., et al. (2009). Earthquakes in Switzerland and surrounding regions during 2008. *Swiss Journal of Geosciences*, 102(3), 505–514. doi:10.1007/s00015-009-1339-8.
- Deichmann, N., & Ernst, J. (2009). Earthquake focal mechanisms of the induced seismicity in 2006 and 2007 below Basel (Switzerland). *Swiss Journal of Geosciences*, 102(3), 457–466. doi:10.1007/s00015-009-1336-y.
- Deichmann, N., & Giardini, D. (2009). Earthquakes induced by the stimulation of an enhanced geothermal system below Basel (Switzerland). *Seismological Research Letters*, 80(5), 784–798. doi:10.1785/gssrl.80.5.784.
- Deichmann, N., Kraft, T., & Evans, K. F. (2014). Identification of faults activated during the stimulation of the Basel geothermal project from cluster analysis and fault mechanisms for the larger magnitude events. *Geothermics*, 52, 84–97. doi:10.1016/j.geothermics.2014.04.001.
- Diehl, T., Deichmann, N., Clinton, J., Husen, S., Kraft, T., Plenkers, K., et al. (2013). Earthquakes in Switzerland and surrounding

- regions during 2012. *Swiss Journal of Geosciences*, 106, 543–558. doi:10.1007/s00015-013-0154-4.
- Diehl, T., Husen, S., Kissling, E., & Deichmann, N. (2009). High-resolution 3-D P-wave model of the Alpine crust. *Geophysical Journal International*, 179, 1133–1147. doi:10.1111/j.1365-246X.2009.04331.x.
- Dreger, D. S. (2003). TDMT INV: Time domain seismic moment tensor INVersion. In Lee, W. H. K., Kanamori, H., Jennings, P. C., and Kisslinger, C. (Eds.), *International Handbook of Earthquake and Engineering Seismology* (Part B). London: Academic Press, pp. 1627.
- Edwards, B., Allmann, B., Fäh, D., & Clinton, J. (2010). Automatic computation of moment magnitudes for small earthquakes and the scaling of local to moment magnitude. *Geophysical Journal International*, 183(1), 407–420. doi:10.1111/j.1365-246X.2010.04743.x.
- Fäh, D., Giardini, D., Bay, F., Bernardi, F., Braunmiller, J., Deichmann, N., et al. (2003). Earthquake catalogue of Switzerland (ECOS) and the related macroseismic database. *Eclogae Geologicae Helveticae Swiss Journal of Geosciences*, 96(2), 219–236.
- Giardini, D., Wiemer, S., Fäh, D., Deichmann, N., Sellami, S., Jenni, S. and the Hazard Team of the Swiss Seismological Service (2004). Seismic Hazard Assessment 2004. *Swiss Seismological Service*, p. 81.
- Hardebeck, J. L., & Shearer, P. M. (2002). A new method for determining first-motion focal mechanisms. *Bulletin of the Seismological Society of America*, 92, 2264–2276.
- Husen, S., Bachmann, C., & Giardini, D. (2007). Locally triggered seismicity in the central Swiss Alps following the large rainfall event of August 2005. *Geophysical Journal International*, 171, 1126–1134. doi:10.1111/j.1365-246X.2007.03561.x.
- Husen, S., Kissling, E., Deichmann, N., Wiemer, S., Giardini, D., & Baer, M. (2003). Probabilistic earthquake location in complex three-dimensional velocity models: Application to Switzerland. *Journal of Geophysical Research*, 108(B2), 2077–2096.
- Kastrup, U., Zoback M.-L., Deichmann, N., Evans, K., Giardini, D., Michael, A. J. (2004). Stress field variations in the Swiss Alps and the northern Alpine foreland derived from inversion of fault plane solutions. *Journal of Geophysical Research*, 109(B1). doi:10.1029/2003JB002550B01402.
- Kastrup, U., Deichmann, N., Fröhlich, A., & Giardini, D. (2007). Evidence for an active fault below the north-western Alpine foreland of Switzerland. *Geophysical Journal International*, 169, 1273–1288. doi:10.1111/j.1365-264X.2007.03413.x.
- Kradolfer, U. and Mayer-Rosa, D. (1988). Attenuation of seismic waves in Switzerland. In: *Recent Seismological Investigations in Europe*. In: *Proceedings of the XIX General Assembly of the European Seismological Commission, Moscow, October 1–6, 1984*, 481–488.
- Lomax, A., Virieux, J., Volant, P., & Thierry-Berge, C. (2000). Probabilistic earthquake location in 3D and layered models. In C. H. Thurber & N. Rabinowitz (Eds.), *Advances in seismic event location* (pp. 101–134). London: Kluwer Academic Publishers.
- Marschall, I., Deichmann, N., & Marone, F. (2013). Earthquake focal mechanisms and stress orientations in the eastern Swiss Alps. *Swiss Journal of Geosciences*, 106, 79–90. doi:10.1007/s00015-013-0129-5.
- Michel, C., Edwards, B., Poggi, V., Burjanek, J., Roten, D., Cauzzi, C., Fäh, D. (2014). Assessment of site effects in Alpine regions through systematic site characterization of seismic stations. *Bulletin of the Seismological Society of America*, 104. doi: 10.1785/0120140097.
- Nanjo, K. Z., Schorlemmer, D., Woessner, J., Wiemer, S., & Giardini, D. (2010). Earthquake detection capability of the Swiss Seismic Network. *Geophysical Journal International*, 181, 1713–1724. doi:10.1111/j.1365-246X.2010.04593.x.
- Pavoni, N. (1977). Erdbeben im Gebiet der Schweiz. *Eclogae Geologicae Helveticae*, 70(2), 351–370.
- Pavoni, N., Maurer, H., Roth, P., & Deichmann, N. (1997). Seismicity and seismotectonics of the Swiss Alps. *Deep structure of the Swiss Alps, results of NRP 20* (pp. 241–250). Basel: Birkhäuser.
- Pavoni, N. & Roth, P. (1990). Seismicity and seismotectonics of the Swiss Alps. Results of microearthquake investigations 1983–1988. In F. Roure, P. Heitzmann & R. Polino (Eds.), *Deep Structure of the Alps*, (Vol. 156, pp. 129–134). Mémoire de la Société géologique de France, Paris.
- Pfiffner, O. A., & Hitz, L. (1997). Geologic interpretation of the seismic profiles of the Eastern Traverse (lines E1–E3, E7–E9): Eastern Swiss Alps. In O. A. Pfiffner, et al. (Eds.), *Deep structure of the Alps, results of NRP20* (pp. 73–100). Basel: Birkhäuser.
- Rüttener, E. (1995). Earthquake hazard estimation for Switzerland. *Matériaux Géologie Suisse, Géophysique*, Nr. 29, Schweizerische Geophysikalische Kommission, ETH-Zürich, p. 106.
- Rüttener, E., Egozcue, J., Mayer-Rosa, D., & Mueller, S. (1996). Bayesian estimation of seismic hazard for two sites in Switzerland. *Natural Hazards*, 14, 165–178.
- Sägesser, R., & Mayer-Rosa, D. (1978). Erdbebengefährdung in der Schweiz. *Schweizerische Bauzeitung*, 78(7), 3–18.
- Singer, J., Diehl, T., Husen, S., Kissling, E., & Duretz, T. (2014). Alpine lithosphere slab rollback causing lower crustal seismicity in northern foreland. *Earth and Planetary Science Letters*, 397, 42–56. doi:10.1016/J.Epsl.04.002.
- Wagner, M., Kissling, E., & Husen, S. (2012). Combining controlled-source seismology and local earthquake tomography to derive a 3-D crustal model of the western Alpine region. *Geophysical Journal International*, 191, 789–802. doi:10.1111/j.1365-246X.2012.05655.x.
- Waldhauser, F., & Ellsworth, W. L. (2000). A double-difference earthquake location algorithm: Method and application to the northern Hayward fault, California. *Bulletin of the Seismological Society of America*, 90(6), 1353–1368. doi:10.1785/0120000006.
- Wiemer, S., Giardini, D., Fäh, D., Deichmann, N., & Sellami, S. (2009). Probabilistic seismic hazard assessment of Switzerland: best estimates and uncertainties. *Journal of Seismology*, 13, 449–478. doi:10.1007/s10950-008-9138-7.
- Ye, S., Ansorge, J., Kissling, E., & Mueller, S. (1995). Crustal structure beneath the eastern Swiss Alps derived from seismic refraction data. *Tectonophysics*, 242, 199–221.